APPENDIX F

SUMMARY OF RECENT INFORMATION RELEVANT TO WASTE FORM DEGRADATION PROCESS MODELS

INTENTIONALLY LEFT BLANK

SUMMARY OF RECENT INFORMATION RELEVANT TO WASTE FORM DEGRADATION PROCESS MODELS

1. INTRODUCTION

This white paper contains a summary of recent test results and other additional information that are relevant to the waste form degradation process model used to support the *Yucca Mountain Science and Engineering Report* (YMS&ER) (DOE 2001a) and the *Yucca Mountain Preliminary Site Suitability Evaluation* (YMPSSE) (DOE 2001b). These two documents were released by the U.S. Department of Energy (DOE) for public review in May and August, respectively, of this year.

The white paper focuses on the results of laboratory tests and other additional information that became available after the waste form degradation process model was completed to support the preparation of the YMS&ER and the YMPSSE. The summary of this recent information is being used to conduct an impact review, in accordance with AP-2.14Q, *Review of Technical Products and Data*, to determine if this additional information has any impact on the technical analyses supporting the YMS&ER and the YMPSSE. The documentation of the additional information in this white paper is an interim step, and primarily used to support this impact review. This information is expected to be formally documented in subsequent Project technical reports, as appropriate.

To assist in the impact review, this white paper briefly describes the waste form degradation process models that were used to support the YMS&ER and the YMPSSE, provides a summary of the recent test results and other additional information, and discusses the potential implications of this more recent information on our understanding of the waste form degradation process model.

2. SUMMARY DESCRIPTION OF THE WASTE FORM DEGRADATION PROCESS MODEL

The waste form degradation models used to support the *Yucca Mountain Science and Engineering Report* (DOE 2001a) and the *Yucca Mountain Preliminary Site Suitability Evaluation* (DOE 2001b) are described in Section 4.2.6 of the *Yucca Mountain Science and Engineering Report* (DOE 2001a). These models estimate, over time, the concentration of dissolved and colloidal radionuclides in any water that may exit the waste package. To do this, the model synthesizes eight major modeling/analysis efforts: radioisotope inventory, in-package chemistry, commercial spent nuclear fuel (CSNF) degradation, commercial CSNF cladding degradation, U.S. Department of Energy (DOE) spent nuclear fuel degradation, high-level radioactive waste degradation, radioisotope dissolved concentration (solubility), and radioisotope colloidal concentration. Of these, significant additional information has been developed for 5 models (1) radionuclide inventory, (2) the degradation rate of CSNF, (3) the surface area of the corroding fuel, (4) the release of colloids from CSNF, and (5) neptunium dissolved concentration limits.

2.1. RADIONUCLIDE INVENTORY

In the *Yucca Mountain Science and Engineering Report* (DOE 2001a), a single inventory for each of the screened-in radionuclides was provided for the average CSNF package by the *Inventory Abstraction* (BSC 2001a). The single inventory was treated as part of the CSNF matrix, to be released contingent upon cladding failure and release from the CSNF matrix. The single-inventory treatment is an approximation because some activity is present outside the CSNF matrix due to neutron activation of mineral deposits and assembly hardware that occurred during reactor operation.

2.2. COMMERCIAL SPENT NUCLEAR FUEL DEGRADATION RATE

The CSNF degradation rate model is based on flow-through tests performed at Pacific Northwest National Laboratory and Lawrence Livermore National Laboratory and is documented in *CSNF Waste Form Degradation: Summary Abstraction* (CRWMS M&O 2000a). This model consists of two equations for the log rate of dissolution, one for acid conditions, and another for alkaline conditions. Statistical analysis of 60 measurements of the rate of dissolution under alkaline conditions showed a complicated dependence of the rate on all varied parameters: temperature, pH, carbonate concentration, oxygen concentration, and fuel burnup. An equation based on the most sensitive parameters: temperature, carbonate concentration, and oxygen concentration was provided to the total system performance assessment (TSPA) with an estimate of error of 1.5 orders of magnitude. The equation for acid conditions was based on one qualified data point combined with a calculated point for pH 7 from the alkaline model, providing an equation as a function of temperature, oxygen concentration and pH. Based on comparison to unqualified data, an error of 1.5 orders of magnitude was assumed for the acid equation.

2.3. COMMERCIAL SPENT NUCLEAR FUEL DEGRADATION SURFACE AREA

The rate of release of soluble radionuclides from a breached CSNF waste package depends, among other factors, on the surface area of the fuel that is exposed to aqueous or humid air environments in the repository. For convenience this area is referred to as the "corroding surface area". The corroding surface area is determined by (1) the extent to which degradation of the fuel cladding compromises the cladding's ability to protect the UO_2 ceramic fuel pellets, and (2) the surface area of the corroding fuel pellets after they are exposed as a consequence of the cladding degradation.

As described in Section 4.2.6.3.3 of the *Yucca Mountain Science and Engineering Report* (DOE 2001a), cladding degradation is assumed to proceed in two distinct steps: (1) perforation of the cladding, and (2) progressive exposure of the uranium dioxide spent nuclear fuel matrix from "wet unzipping" i.e., a process which results in tearing or splitting of the cladding. The experimental results described below in Section 3.3 address the latter step and the evolution of the surface area of the corroding fuel pellets when they are exposed as a consequence of cladding unzipping.

The "wet unzipping model" for the progression of cladding failure following an initial breach is described in *Clad Degradation–Wet Unzipping* (CRWMS M&O 2000b) and the model parameter values are discussed in the *Yucca Mountain Science and Engineering Report*

(DOE 2001a) and Volume 1 of *FY01 Supplemental Science and Performance Analyses* (BSC 2001b). The rate of propagation of the axial unzipping of the cladding is related to the rate of corrosion of the fuel. The corroding surface area of the fuel is represented as a cone shaped area whose height is determined by the ratio of unzipping speed to corrosion rate.

2.4. RELEASE OF COLLOIDS FROM COMMERCIAL SPENT NUCLEAR FUEL

The release of waste form colloids from the CSNF drip tests at Argonne National Laboratory was insignificant relative to other sources of colloids and was not included in colloid release modeling.

2.5. NEPTUNIUM CONCENTRATIONS

As discussed in Volume 1, Section 9.3.2.2.3 of *FY01 Supplemental Science and Performance Analyses* (BSC 2001b), the solid phases that may control the dissolved concentration of Np are uncertain. The models used for the dissolved Np concentration were based on the solubility of pure neptunium phases, as described in the *Yucca Mountain Science and Engineering Report* (DOE 2001a). Subsequently, based on observations from unsaturated tests, an empirical model based on co-precipitation of neptunium in the U(VI) compound schoepite was developed. This model is described in Volume 1, Section 9.3.2.2.3 of *FY01 Supplemental Science and Performance Analyses* (BSC 2001b). Because the specific phases that will control the dissolved concentration of neptunium as spent nuclear fuel corrodes remain uncertain, the abstracted model spanned a broad uncertainty range as described in *FY01 Supplemental Science and Performance Analyses*.

3. SUMMARY OF RECENT TEST RESULTS AND OTHER ADDITIONAL INFORMATION

This section summarizes recent results obtained from laboratory tests and modeling efforts that have provided information relevant to enhancing understanding of the waste form degradation process model. The additional information is listed below and discussed in each of the subsections that follow.

1. Refinement of location of radionuclide inventory
2. Flow-through CSNF dissolution rate measurements
3. Tests of commercial spent nuclear fuel rod segments exposed to humid air at 175°C (347°F)
4. CSNF colloid generation tests
5. Tests to evaluate Np incorporation into uranyl alteration phases.

Because of the recent nature of the information provided in this section, much of it is unpublished and, therefore, some source references have been provided where appropriate, but others could not be provided. However, this information is currently documented in the principal

investigators' scientific notebooks, if applicable, in accordance with the Project's quality assurance procedure AP-SIII.1Q, *Scientific Notebooks*.

3.1. REFINEMENT OF LOCATION OF RADIONUCLIDE INVENTORY

A recent reexamination of the radionuclide inventory calculations (CRWMS M&O 1999a; CRWMS M&O 1999b) found that the approximation is a good one for all radionuclides except C-14. (This reexamination will be documented in a revision of *Inventory Abstraction* [BSC in preparation].) Assembly hardware components (primarily stainless steel components in the top and bottom regions of the assemblies) account for a substantial fraction (about one-fifth) of the total CSNF C-14 inventory. Degradation times ranging from about 100 to about 1,000 years after waste package breach are estimated for the stainless steel components. Because the C-14 from the stainless steel may be released much sooner than the bulk of the C-14 from the CSNF matrix, separating out the inventory of C-14 from CSNF hardware-activation products may result in an increased early release of C-14.

3.2. COMMERCIAL SPENT NUCLEAR FUEL DISSOLUTION

A systematic study was undertaken to measure the accuracy and reproducibility of the flow-through testing of CSNF that has been performed at Pacific Northwest National Laboratory. These flow-through tests were designed to operate under relatively high flow conditions to avoid solubility concerns and prevent back reactions, thus providing an upper bound for release of radionuclides.

An examination of the raw data has shown that pH is very difficult to control for many of these tests. While a constant value for pH is assumed and utilized for determining the dissolution rate dependence on pH, in reality the pH for some tests varied by as much as ±0.5. The pH dependence in the AMR is weak under alkaline conditions, so the impact on the data and model is minimal.

Flow through testing has been performed on unirradiated UO_2 and well-characterized commercial fuels: accepted test material 103 (ATM-103), a moderate burnup (~30 GWd/MTHM) PWR fuel; ATM-106, a moderate burnup (~43 GWd/MTHM) PWR fuel; and ATM-109, a high burnup (~70 GWd/MTHM) BWR fuel. Burnup of fuel causes changes in the physical, chemical, and radiological properties of the fuel, which are not uniform across the fuel. It was therefore not surprising that burnup was one of the parameters that showed a complicated effect on dissolution rate, showing its largest effects in cross terms with the other parameters such as temperature. An expert panel (CRWMS M&O 1998) proposed a dissolution equation using only oxygen, carbonate and temperature. This approach was used in the TSPA abstraction. Burnup was reexamined to better understand its uncertainty. An attempt was made to segregate the high burnup rim from the center of the ATM-109 fuel. However, the washing process most likely resulted in the fine-grained rim material being washed away. Examination of scanning electron microscope images of the fuels reveals little, if any, rim material in the sample. Thus, there is virtually no difference reported between the rim material and the bulk, reducing the net burnup of the sample up to 20 GWd/MTHM. For the lower burnup fuels, the washing process was estimated to introduce an uncertainty in burnup of up to 5 GWd/MTHM. To further test the potential for biasing a sample's initial inventory, a new method of crushing and sieving

the fuel was devised. A comparison of the measured surface area of fuel prepared using this method and fuel that was crushed, sieved, and washed, as was done for all samples used in the model development, clearly demonstrated that the new method produced a sample with a surface area almost one order of magnitude higher. While this may be due to the crushing technique, an additional test was designed to examine sample biasing. The washed samples contained up to a factor of two less cesium than the unwashed samples. Similarly, the smaller particles from the unwashed fuel contained higher cesium concentrations than the larger particles. It thus appears that washing may have biased samples by up to a factor of two by eliminating small particles in addition to fines. The uncertainty in effective burnup of the samples used in the regressions due to the crushing, sieving, and washing procedure may have contributed to the complicated regression equations obtained. Since burnup was not used in the equation used by TSPA, it contributed to the estimated uncertainty used in TSPA.

An examination of the Pacific Northwest National Laboratory record books containing the data for the flow-through tests revealed that many of the collected leachates resulted in occasional high uranium concentrations, as much as one to three orders of magnitude higher than other leachates from the same series. These data points were considered to be contaminated due to either activity in the hot cell or release of fuel particles through the 0.5 μm frits and were not included in determining the dissolution rate of that sample. A number of archived leachates from CSNF flow-through tests were reanalyzed for total uranium concentration after the samples had been stored in glass vials under acidic conditions (pH~1) over times ranging from a few months to a few years. In every case, the total uranium concentration was greater than the original value. The increases were more than could be accounted for by leaching of uranium from the glass vials. The uranium concentration for these samples averaged about 20 percent higher than the original value. While this is small compared to the uncertainty in the model abstraction, it clearly indicates that the reported numbers to date may not have accounted for all uranium released from a flow-through test. A similar experiment was performed on some mixed-oxide fuels tested by the National Spent Nuclear Fuel Program. The results showed an even higher increase in total uranium content, with some samples exhibiting increases by a factor of 2, 5, and 22. Initial tests to determine if uranium was released in the +4 oxidation state, and hence would not be observed by the kinetic phosphorescence analysis method utilized, showed only U^{+6}. The leachates and standards were then tested using inductively-coupled plasma-mass spectroscopy. While the standards showed excellent agreement between kinetic phosphorescence analysis and inductively-coupled plasma-mass spectroscopy, the test leachates were consistently 20 percent lower for the inductively-coupled plasma-mass spectroscopy. This suggests a possible matrix interference or background stripping error that needs to be examined. A recent finding from the Savannah River Site, where flow-through testing on unirradiated Al-based fuels were performed, suggests they did not utilize frits, or may have had much larger frit openings, than similar tests at Pacific Northwest National Laboratory, thereby accounting for the order of magnitude difference in reported dissolution rates. It thus appears likely that particulate or colloidal release from flow-through tests may be on the order of at least 20 percent of the total release. While this amount is small relative to the total uncertainty associated with the dissolution rate model, it may be significant in terms of colloid formation and release. Since these tests were used to predict the rate of dissolution and not the rate of fuel erosion, the fact that the colloids were not detected may be fortuitous.

Results from recent experiments at Pacific Northwest National Laboratory have suggested that hydrated phases of uranium form quite rapidly, but may be unstable. The results of flow-through testing on DOE spent nuclear fuels as part of the National Spent Nuclear Fuel Program also suggest a "cyclic" release of uranium during those tests. To test this hypothesis, X-ray diffraction was performed on some of the CSNF from recently finished tests. One of the samples exhibited a very strong schoepite (UO_3-$2H_2O$) peak. Additionally, the columns and drip tubes from the terminated tests were rinsed with acidified water. The collected leachates exhibited relatively larger uranium concentrations, although some residual fuel may have adhered to the column or frits. However, plate-out of uranium in the system is a concern but will have minimal impact on the uncertainty in the model abstraction.

The dissolution rate is directly dependent on the surface area of the fuel being tested. The surface area has been determined using the BET method. An examination of Table 3.3-1 in the *Waste Form Degradation Process Model Report* (CRWMS M&O 2000c) shows, in at least one case (runs #22 and 28), that fuels tested under identical conditions had dissolution rates that differed by more than a factor of two. From Table 2 of *Spent Fuel Dissolution Rates as a Function of Burnup and Water Chemistry* (Gray 1998), it is clear that this difference is readily attributed to the difference in measured surface area. While the difference may be real, it is necessary at this time to assume that the BET method for measuring surface area has an uncertainty of at least a factor of two and that this uncertainty contributed to the overall uncertainty of the dissolution rate. The procedure has been refined and a National Institute of Standards and Technology-traceable standard has been obtained to better quantify this uncertainty for all future tests.

3.3. TESTING OF COMMERCIAL SPENT NUCLEAR FUEL ROD SEGMENTS ON EXPOSURE TO HUMID AIR

The results described here were obtained from tests designed to examine the behavior of fuel rod segments with breached cladding upon extended exposure to humid air at 175°C (347°F). The tests were performed at 175°C (347°F) to accelerate the oxidative dissolution of the fuel so that mechanisms that can potentially lead to cladding unzipping could be observed in a reasonable time frame. The results discussed here were obtained from two test samples each consisting of ~2.5-cm (3.5-in.) segments of ATM-103. The samples were capped at each end with titanium Swagelok caps to confine the fuel and reaction products. Each end cap and the cladding of each sample had 2-mm (0.08-in.) drilled holes to simulate how a cladding defect might allow the fuel pellets to react in a fuel rod with breached cladding. The samples were sealed in 316 stainless steel vessels with a quantity of water sufficient to produce an environment of 100 percent relative humidity (about 0.4 to 1.01 mL).

As shown in Figure 1 visual examination of one of the samples at 541 days into the test revealed that it had developed an axial crack that passed through the drilled hole in the cladding and ran the full length of the sample. This crack had developed since the sampling about 7 months earlier. This unzipping speed is faster than the range used in the YMS&ER (DOE 2001a) and is consistent with the upper bound used in the supplemental TSPA model.

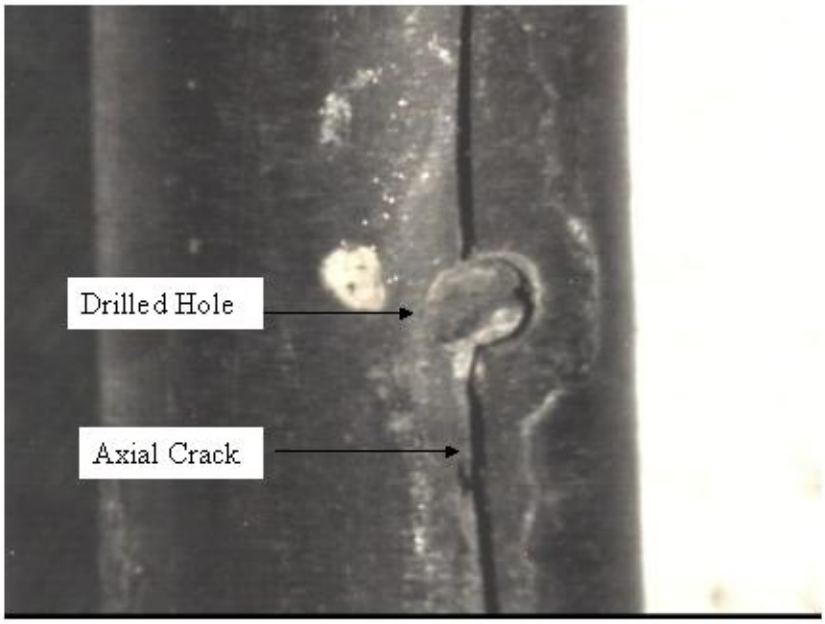

Figure 1. Picture of Fuel Rod Sample Showing Axial Crack Passing Through the Drilled Hole in the Cladding

The second sample also showed a similar axial crack, although it was less apparent at 541 days into the test.

Subsequent transverse sectioning of the first sample showed evidence of infilling of the fractures and the gap between the fuel and the cladding with alteration phases as shown in Figure 2a. The transverse sectioning also showed evidence for alteration of the cladding and the fuel immediately adjacent to the fracture opening as shown in Figure 2b.

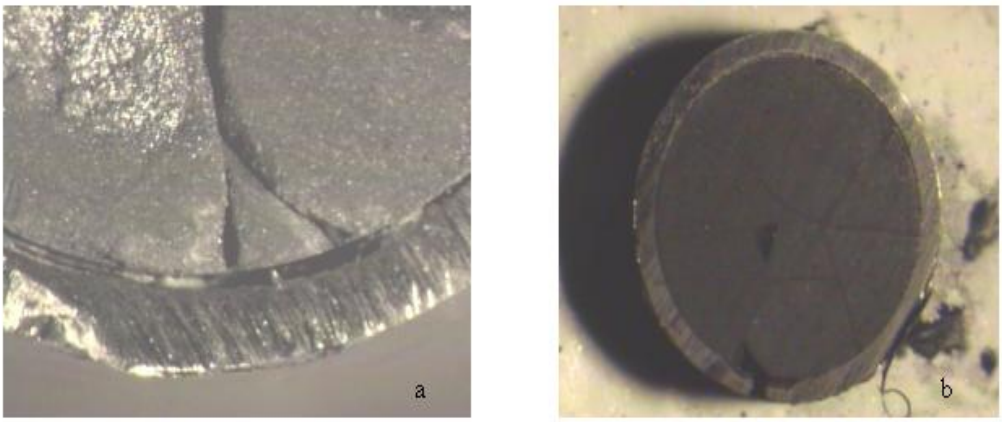

Figure 2. Images of As-Cut Sections of the Fuel Sample Showing Infilling of the Gap Between the Fuel and the Cladding (a) and the apparent thinning of the cladding adjacent to the fracture opening (b).

After the fuel pellets are exposed as a consequence of cladding unzipping, the rate of radionuclide release is determined, in part, by the surface area of the fuel matrix that is available for corrosion. Microscopic examination of corroded CSNF has shown evidence for preferential corrosion of the fuel matrix along grain boundaries (Finch et al. 1999). This observation raises questions about how the associated increase in the corroding surface area of the fuel might influence the rate of radionuclide release as the corrosion process progresses.

The effect of grain boundary corrosion on radionuclide release from corroding fuel can be inferred from the rate of radionuclide release observed in long-term unsaturated "drip" tests. In these tests fuel pellets fragments are exposed to humid air and periodic injection of simulated groundwater at 90°C (194°F). After more than eight years of reaction, the fuel pellet fragments are covered by a thick layer of uranyl alteration products as illustrated in Figure 3. This observation is consistent with a general corrosion process that involves oxidative dissolution of the fuel matrix and precipitation of uranyl alteration phases at the outer surfaces of the corroding fuel.

Figure 3. Visual Appearance of Fragments of the ATM-103 Fuel after 8.2 Years of Exposure to Humid Air and Dripping Groundwater

The long-term release rate of soluble radionuclides such as ^{99}Tc in the drip tests is also consistent with the general corrosion process outlined above in which most of the corrosion of the fuel matrix occurs at the outer surface. Figure 4 shows the release of ^{99}Tc for the ATM-103 and ATM-106 fuels.

These data show that the release rate of ^{99}Tc exhibits a generally decreasing trend with time. This may be due to depletion of Tc that is preferentially located at grain boundaries. However, this behavior also indicates that, if preferential grain boundary corrosion progresses with time, there is no evidence that it manifests itself in increased release of soluble elements (e.g., Tc-99) from the fuel under the long-term drip test conditions.

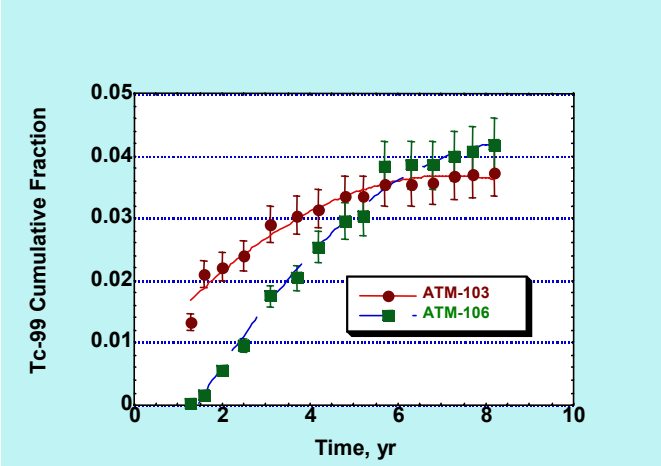

Figure 4. Observed ^{99}Tc Release from ATM-103 and ATM-106 Spent Nuclear Fuel Under Unsaturated Drip Test Conditions

3.4. COMMERCIAL SPENT NUCLEAR FUEL COLLOID GENERATION TESTS

Because earlier samplings of the CSNF drip tests indicated that little, if any, Pu colloids were formed under the test conditions, changes were made to the experimental configuration to check if this result might be an artifact of the test configuration. Specifically, the potential effect of retainer hole size (the retainer is the base of the fuel holder) on holdup of Pu colloids was examined for the ATM-103 and ATM-106 test intervals ending at 88 and 92 months. After 82 months of reaction, a new Zircaloy-4 retainer containing 10-µm holes was used in both of these tests. After 88 months, the Zircaloy-4 retainer was replaced with a gold mesh retainer with 200-µm holes (Note: the 200-µm holes were used to avoid the possibility of colloid filtration. However, these larger holes also increase the possibility of particulates being entrained in the leachate). The concentrations of Pu in the leachate that were filterable using filters with 450 and 5 nm pores were determined when these tests were sampled at 88 and 92 months and are summarized in Table 1. Also shown in Table 1 are the "dissolved" (i.e., the Pu concentration that was not filtered by the 5-nm pore size filter) and the "sorbed" concentration (i.e., the amount of Pu removed from the vessel walls by acid stripping divided by the volume of the leachate). For comparison, the recent results for the ATM-109A and ATM-109C high-drip tests, which used a Zircaloy-4 retainer with 10-µm holes, are also presented in Table 1.

The results in Table 1 show that both the dissolved and colloidal Pu concentrations in the leachate are very small indeed even after the hole size in the fuel retainer was changed to minimize possible colloid filtration. Results from dynamic light scattering analysis of aliquots of the collected leachate and examination of transmission electron microscope grids prepared by wicking a drop of the leachate through a "holey" carbon grid also showed that the leachate contained few colloids and the few that were observed on the transmission electron microscope grids did not contain uranium-phase substrates. The appearance of the fuel and the associated alteration phases suggests that the alteration phases may limit colloid formation by promoting precipitation at the fuel surface as opposed to homogenous nucleation and precipitation in the leachate. This might explain the small Pu colloid concentrations observed (Table 1) and the

apparent absence of uranium-phase substrates in the few colloids that were observed. However, as shown in Table 1, the "sorbed" Pu concentration can be many orders of magnitude larger than the measured Pu colloid concentration in the leachate. This result may be due to the transport of fuel or alteration phase particles through the holes in the base of the fuel holder and the subsequent settling or deposition of these particles onto the test vessel walls. Alternatively, it is also possible that the sorbed Pu represents Pu colloids that are deposited onto the stainless steel vessel walls as the leachate accumulates in the test vessel. Thus the actual Pu colloid concentration could include the Pu sorbed concentration shown in Table 1. (Note: If Pu colloids are indeed the source of the sorbed Pu the results indicate that these colloids are unstable with respect to deposition onto the stainless steel vessel walls under the test conditions.) An important objective of the continuing experimental work is to discriminate between the possible explanations for the "sorbed" Pu concentrations.

Table 1. Recent Pu Colloid Data for High-Drip Fuel Fragment Tests

Test Interval	Pu Sorbed (M)	Pu Dissolved (M)	Pu Particulate (M)	Pu Colloid (M)	Pu Total Release (M)
ATM-103 88mo[a]	4E-8	4E-10	3E-10	2E-9	4E-8
ATM-103 92mo[b]	8E-7	ND[d]	7E-9	3E-10	8E-7
ATM-106 88 mo[a]	4E-7	2E-10	ND	6E-10	4E-7
ATM-106 92 mo[b]	2E-6	BD	1E-9	2E-10	2E-6
ATM-109A 19mo[c]	5E-10	1E-10	4E-12	6E-10	1E-9
ATM-109A 23mo[c]	8E-10	ND	ND	4E-11	8E-10
ATM-109C 19mo[c]	1E-8	8E-11	8E-10	2E-9	1E-8
ATM-109C 23mo[c]	3E-8	ND	9E-10	ND	3E-8

[a] New Zircaloy-4 retainer with 10-μm holes was used in this interval.

[b] Gold mesh retainer with 200-μm holes was used in this interval.

[c] Original Zircaloy-4 retainer with 10-μm holes was used in this interval.

[d] ND = Not detected; below inductively-coupled plasma-mass spectroscopy detection limits.

3.5. TESTING TO EVALUATE NP INCORPORATION INTO URANYL ALTERATION PHASES

As pointed out in Section 2, the solid phases that control the dissolved concentration of neptunium as CSNF corrodes remain uncertain. This uncertainty is due to very limited experimental observations of the solid phases that may limit the dissolved concentrations of neptunium as CSNF corrodes (BSC 2001b, Section 9.3.2.2.3).

Because of the slow corrosion rates of CSNF and the very low mass fractions of neptunium in the CSNF fuel matrix (~0.00194, see BSC 2001b, p. 9-13), it is not practical to experimentally investigate the phases that may control Np behavior using CSNF corrosion studies alone. In order to study the behavior of Np during the corrosion of Np-bearing U solids, a series of tests on the corrosion of Np-doped U oxides was begun. Because the oxidative corrosion of UO_2 is slow on laboratory timescales, the corrosion of the Np-bearing solids was accelerated by synthesizing U oxides in which the U is already oxidized beyond U(IV). The initial experimental work focused on synthesizing a homogeneous uranium oxide for use in "accelerated" corrosion tests (i.e., tests that would achieve results within a few months or less). The uranium oxide chosen for testing is U_3O_8, and homogenous single-phase Np-doped U_3O_8 with a wide range of Np:U ratios

(1:8 ≤ Np:U ≤ 1:160) has been successfully synthesized for use in these tests. To facilitate experimental identification of the solid alteration phases, the initial corrosion tests have focused on Np-doped U_3O_8 with Np:U ratios near the upper end of this range.

Tests on the corrosion of Np-doped U_3O_8 have been performed in sealed stainless-steel vessels in air saturated with water vapor at 90° and 150°C (194° and 302°F). Early results demonstrate that U_3O_8 corrodes under these conditions to form a variety of uranium(VI) solids, depending on temperature. Dehydrated schoepite, $(UO_2)_4O_{0.25-x}(OH)_{1.75+2x}$, forms at both test temperatures, whereas metaschoepite, $(UO_2)_4O(OH)_6(H_2O)_5$, is found only in tests conducted at 90°C (194°F). In addition, under the test conditions, the corrosion of U_3O_8 doped with a sufficiently high concentration of Np (Np:U = 1:8) results in the precipitation of crystalline NpO_2 at 90° and 150°C (194° and 302°F); crystalline Np_2O_5 also forms at 90°C (194°F). The uranium and neptunium phases observed in these tests are summarized in Table 2 and are illustrated in Figures 5 and 6. Figure 7 shows the X-ray powder patterns.

Table 2. Solids Identified from Corrosion Tests on Np-Doped U_3O_8

Temperature (duration)	Np:U	
	1:8	1:80
150°C (2-4 weeks)	DS, NpO_2	DS, NpO_2
90°C (16 weeks)	DS, MS, NpO_2, Np_2O_5	DS, MS

NOTE: DS = dehydrated schoepite; MS = metaschoepite; U_3O_8 is also present in all samples analyzed.

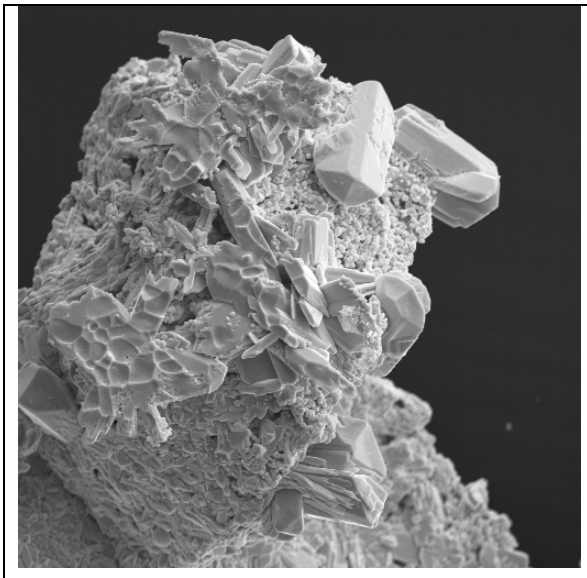

Figure 5a. Secondary-Electron Image of Dehydrated Schoepite Crystals on Np-Doped U_3O_8. Note the field of Np-rich spheres at upper right. Field of view is ~390 micrometers across.

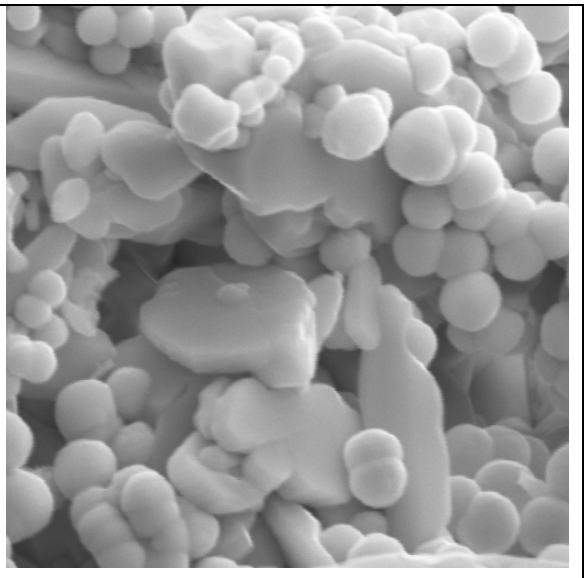

Figure5b. Secondary-Electron Image of Np-Rich Spheres and Crystals of Dehydrated Schoepite. Field of view is ~30 micrometers across.

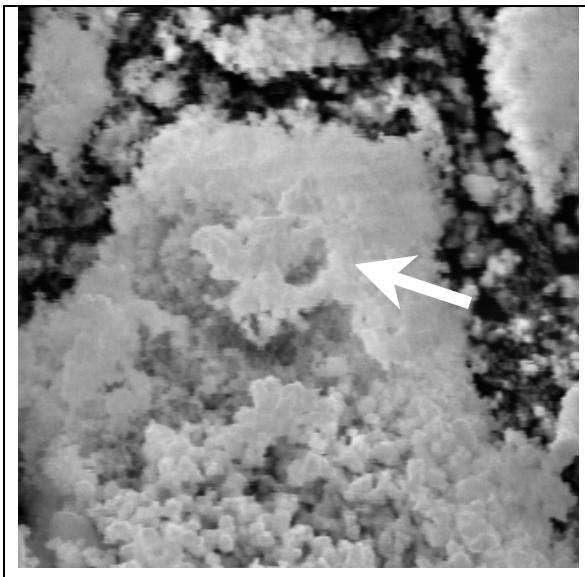

Figure 6a. Secondary-Electron Image of Altered Np-Doped U_3O_8 (Np:U = 1:8) Following Reaction in Humid Air for 16 Weeks at 90°C. Qualitative chemical analysis by electron dispersive spectroscopy of the region indicated by the arrow reveals a high Np concentration.

Field of view is 0.03 mm across.

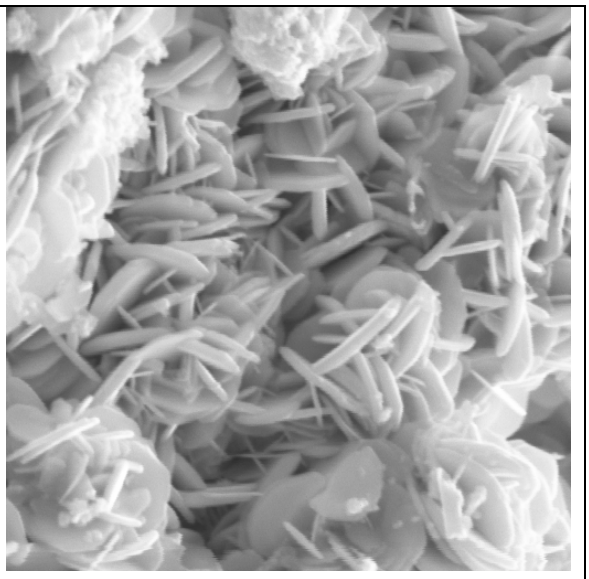

Figure 6b. Secondary-Electron Image of Metaschoepite Crystals on the Surface of Altered Np-Doped U_3O_8 (Np:U = 1:80) Following Reaction in Humid Air for 16 Weeks at 90°C.

Field of view is ~0.03 mm across.

Observation of the precipitation of crystalline NpO_2 from Np-doped U_3O_8 under nominally oxidizing conditions strongly suggests that thermodynamically based predictions of NpO_2 stability are correct (for 150°C [302°F]), and that a solid with some reduced U effectively reduces (or keeps reduced) Np and permits NpO_2 precipitation under the experimental conditions. The (tentative) identification of crystalline Np_2O_5 under experimental conditions similar to the 150°C (302°F) runs, but at 90°C (194°F), demonstrates that the experiments are sufficiently oxidizing to stabilize this Np(V) solid, at least transiently.

The tentative identification of Np_2O_5 in the tests conducted at 90°C (194°F), especially coexisting with NpO_2, raises several questions. Of primary interest is whether the two coexisting Np oxides reflect a thermodynamic equilibrium between two solids with different Np oxidation states, or whether one of the Np oxides is a kinetic product that will (eventually) convert to the thermodynamically stable solid. Current thermodynamic data indicate that NpO_2 is the stable Np-bearing solid in equilibrium with water and air.

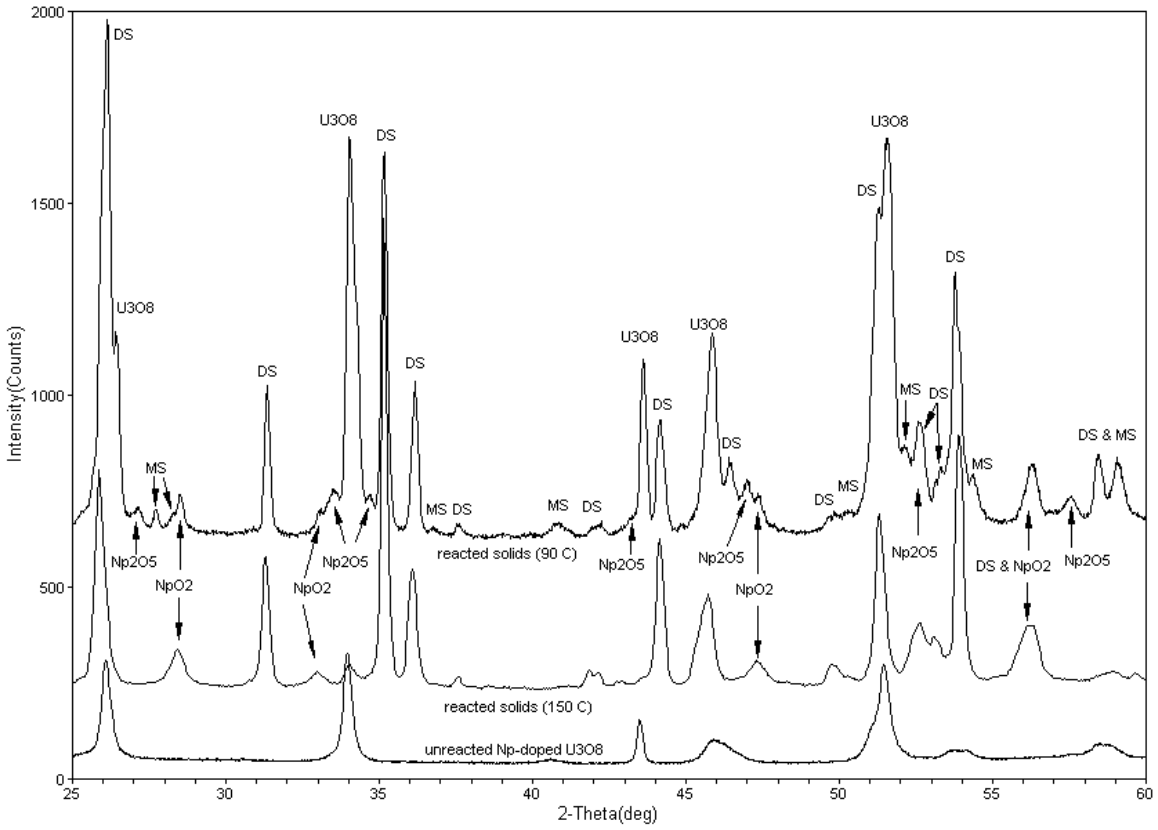

Figure 7. X-Ray Powder Patterns of Np-Doped U_3O_8 (Np:U = 1:8) Before Reaction in Humid Air (bottom) and Reacted Solids after Sixteen Weeks of Reaction at 90°C (top). X-ray diffraction powder pattern for Np-doped U_3O_8 reacted at 150°C is also shown for comparison (middle). Peaks corresponding to dehydrated schoepite (DS), metaschoepite (MS), as well as those tentatively assigned to Np_2O_5 and NpO_2, are indicated in the X-ray diffraction powder pattern for the reacted solids. Note the absence of peaks for metaschoepite, dehydrated schoepite, Np_2O_5, and NpO_2 in the pattern from the unreacted U_3O_8, demonstrating that these solids formed as alteration products in the corrosion tests.

4. IMPLICATIONS OF RECENT TEST RESULTS AND OTHER ADDITIONAL INFORMATION

4.1. INVENTORY

Up to about one fifth of the C-14 inventory is in the stainless steel assembly hardware components and not protected by the fuel cladding. Because the C-14 from the stainless steel may be released much sooner than the bulk of the C-14 from the CSNF matrix, separating out the inventory of C-14 from CSNF hardware-activation products may result in an increased early release of C-14.

4.2. COMMERCIAL SPENT NUCLEAR FUEL DISSOLUTION TESTING

Within the stated uncertainty, the model dissolution rate is adequate for its stated purpose: a bounding model for use in the TSPA-SR and supplemental TSPA.

4.3. TESTING OF COMMERCIAL SPENT NUCLEAR FUEL ROD SEGMENTS ON EXPOSURE TO HUMID AIR

The initial destructive examination results described above indicate that the progression of the alteration of the fuel pellets in breached fuel is consistent with the conceptual basis for the unzipping model. The alteration of the fuel produces alteration phases that fill the gap between the fuel pellets and the cladding and also the fuel fracture openings. The expected alteration phases and how they are expected to exert hoop stresses on the cladding that may lead to axial unzipping are described in *Clad Degradation—Wet Unzipping* (CRWMS M&O 2000b). The results presented here show that, regardless of the mechanisms involved, the corrosion reactions taking place inside the cladding can exert hoop stresses on the cladding and produce axial cracking under the laboratory test conditions involved. The unzipping observed in these tests was faster than the range used in TSPA-SR model described in the YMS&ER (DOE 2001a) and is consistent with the upper bound used in the supplemental TSPA model described in *FY01 Supplemental Science and Performance Analyses* (BSC 2001b).

4.4. COMMERCIAL SPENT NUCLEAR FUEL COLLOID GENERATION

New drip testing indicates that if colloidal or particulate fuel fragments are released that they are likely to stick to the stainless steel internal components. The net result is that negligible amounts of CSNF colloids are expected to be released under low flow conditions as modeled in the TSPA-SR and supplemental TSPA models.

4.5. TESTING TO EVALUATE NP INCORPORATION INTO URANYL ALTERATION PHASES

The experimental results show that NpO_2, Np_2O_5, dehydrated schoepite, and metaschoepite can form in the corrosion of neptunium-doped U_3O_8. This suggests that the dissolved concentration of Np in contact with corroding CSNF may be limited by one or more of these phases. In the bounding TSPA-SR model, Np_2O_5 was the assumed controlling phase, but in the supplemental TSPA coprecipitation of Np with dehydrated schoepite or metaschoepite was also considered. The new results also indicate that it is appropriate to use a model for dissolved concentrations of neptunium that spans the solubility behavior of all these phases pending additional experimental results that identify the specific phases that are likely to control the dissolved neptunium concentrations.

5. REFERENCES

AP-2.14Q, REV 2, ICN 0. *Review of Technical Products and Data*. Washington, D.C.: U.S. Department of Energy, Office of Civilian Radioactive Waste Management.
ACC: MOL.20010801.0316.

AP-SIII.1Q, Rev. 0, ICN 1. *Scientific Notebooks*. Washington, D.C.: U.S. Department of Energy, Office of Civilian Radioactive Waste Management. ACC: MOL.20000516.0002.

BSC (Bechtel SAIC Company) 2001a. *Inventory Abstraction.* ANL-WIS-MD-000006 REV 00 ICN 02. Las Vegas, Nevada: Bechtel SAIC Company. ACC: MOL.20010416.0088.

BSC 2001b. *FY01 Supplemental Science and Performance Analyses, Volume 1: Scientific Bases and Analyses.* TDR-MGR-MD-000007 REV 00 ICN 01. Las Vegas, Nevada: Bechtel SAIC Company. ACC: MOL.20010801.0404; MOL.20010712.0062; MOL.20010815.0001.

BSC (in preparation). *Inventory Abstraction.* ANL-WIS-MD-000006 REV 00 ICN 03. Las Vegas, Nevada: Bechtel SAIC Company.

CRWMS M&O (Civilian Radioactive Waste Management System Management and Operating Contractor) 1998. *Waste Form Degradation and Radionuclide Mobilization Expert Elicitation Project.* Las Vegas, Nevada: CRWMS M&O. ACC: MOL.19980804.0099.

CRWMS M&O 1999a. *BWR Source Term Generation and Evaluation.* BBAC00000-01717-0210-00006 REV 01. Las Vegas, Nevada: CRWMS M&O. ACC: MOL.20000113.0334.

CRWMS M&O 1999b. *PWR Source Term Generation and Evaluation.* BBAC00000-01717-0210-00010 REV 01. Las Vegas, Nevada: CRWMS M&O. ACC: MOL.20000113.0333.

CRWMS M&O 2000a. *CSNF Waste Form Degradation: Summary Abstraction*. ANL-EBS-MD-000015 REV 00. Las Vegas, Nevada: CRWMS M&O. ACC: MOL.20000121.0161.

CRWMS M&O 2000b. *Clad Degradation—Wet Unzipping*. ANL-EBS-MD-000014 REV 00. Las Vegas, Nevada: CRWMS M&O. ACC: MOL.20000502.0398.

CRWMS M&O 2000c. *Waste Form Degradation Process Model Report.* TDR-WIS-MD-000001 REV 00 ICN 01. Las Vegas, Nevada: CRWMS M&O. ACC: MOL.20000713.0362.

DOE (U.S. Department of Energy) 2001a. *Yucca Mountain Science and Engineering Report.* DOE/RW-0539. Washington, D.C.: U.S. Department of Energy, Office of Civilian Radioactive Waste Management. ACC: MOL.20010524.0272.

DOE 2001b. *Yucca Mountain Preliminary Site Suitability Evaluation.* DOE/RW-0540. Washington, D.C.: U.S. Department of Energy, Office of Civilian Radioactive Waste Management. ACC: MOL.20011101.0082.

Finch, R.J.; Buck, E.C.; Finn, P.A.; and Bates, J.K. 1999. "Oxidative Corrosion of Spent UO_2 Fuel in Vapor and Dripping Groundwater at 90°C." *Scientific Basis for Nuclear Waste Management XXII, Symposium held November 30-December 4, 1998, Boston, Massachusetts, U.S.A.* Wronkiewicz, D.J. and Lee, J.H., eds. *556,* 431-438. Warrendale, Pennsylvania: Materials Research Society. TIC: 246426.

Gray, W.J. 1998. *Spent Fuel Dissolution Rates as a Function of Burnup and Water Chemistry.* PNNL-11895. Richland, Washington: Pacific Northwest National Laboratory. ACC: MOL.19980612.0161.